NUMERICAL SIMULATIONS OF INDIAN OCEAN TSUNAMI BY TUNA-M2

Cham Kah Loon, Teh Su Yean, [1]Koh Hock Lye, [2]Ahmad Izani Md Ismail
School of Mathematical Sciences, Universiti Sains Malaysia, 11800 USM, Penang.
e-mail: [1]hlkoh@cs.usm.my, [2]izani@cs.usm.my

Abstract. *The Sumatra-Andaman earthquake of magnitude 9.3 on the Richter scale occurred on 26 December 2004. It triggered off a series of tsunami waves that caused tremendous damage to the properties and lives along the affected coastal areas. The earthquake was located where the India Plate dives under the Burma Plate, and was extremely large in geographical extent, beginning off the coast of Aceh and proceeding northwesterly over a period of about 100 seconds. An estimated fault length is about 800 km, with a fault width of about 85 km and an initial vertical displacement of 11 m. There were no tsunami warning systems in the Indian Ocean to detect tsunamis, nor to warn the general populace living around the ocean. Thus, there is a need for early warning systems to predict the characteristics of tsunami propagation, including tsunami wave heights and arrival times. There are three phases of tsunami evolution, which are generation, propagation and runup. Tsunami is generated by the disturbance associated with seismic activity, explosive volcanism, and submarine landslide phenomena. Propagation of tsunami waves transports seismic energy away from the earthquake source. During the deep ocean propagation stage, the wave height is small compared to the wavelength and the ocean depth. Therefore, the linear wave theory can be applied. Tsunami runup is the most destructive phase of tsunami evolution. The wave behavior at the shoreline depends on such characteristics as the relationships between wavelength and water depth and between the wavelength of the wave and its height. This paper will present the simulations of these tsunami propagations in the Indian Ocean and discuss wave height characteristics near the coast of Sri Lanka, Bangladesh and India to highlight tsunami hazards and coastal vulnerability. The need for an early warning system in the Indian Ocean would appear urgent. The simulation is performed by means of an in-house tsunami numerical simulation model TUNA-M2 that solves the shallow water equation by the staggered finite difference method.*

1 Introduction : Tsunami numerical models

There are several numerical models available for simulating the propagation of tsunami waves. TUNAMI-N2 developed by Imamura of Tohoku University [2] is one of these models. Another well-known model is the method of splitting tsunami model (MOST) developed by Titov and Gonzalez [12]. The MOST model, which will be used to develop tsunami hazard mitigation tools for the Pacific Disaster Center (PDC) has been used successfully to simulate the tsunami generation by a source near Alaska, propagation across the Pacific Ocean, and subsequent runup onto the Hawaiian shoreline. However, TUNAMI-N2 and MOST models will not be used in this paper. An in-house tsunami propagation model in two dimensions, TUNA-M2 will be used in this paper. The relevant features and characteristics of tsunami propagations in deep oceans are simulated by means of TUNA-M2.

2 TUNA-M2 model

TUNA-M2 is developed based upon the shallow water equations (SWE) [11]. This model has been used to simulate the propagation of the Dec 26, 2004 tsunami waves towards the coastal regions of Malaysia and Thailand [7, 15]. An enhancement of the open sea boundary condition has been implemented for TUNA-M2 to improve its capability for the current paper.

2.1. Shallow Water Equations (SWE)

Under certain assumptions typically applicable to tsunami propagation in the ocean, hydrodynamic equations that describe the conservation of mass and momentum can be depth averaged [1]. They can be written in flux form [3, 4] as follow.

$$\frac{\partial \eta}{\partial t} + \frac{\partial M}{\partial x} + \frac{\partial N}{\partial y} = 0 \quad (1)$$

$$\frac{\partial M}{\partial t}+\frac{\partial}{\partial x}\left(\frac{M^2}{D}\right)+\frac{\partial}{\partial y}\left(\frac{MN}{D}\right)+gD\frac{\partial \eta}{\partial x}+\frac{gn^2}{D^{7/3}}M\sqrt{M^2+N^2}=0 \quad (2)$$

$$\frac{\partial N}{\partial t}+\frac{\partial}{\partial x}\left(\frac{MN}{D}\right)+\frac{\partial}{\partial y}\left(\frac{N^2}{D}\right)+gD\frac{\partial \eta}{\partial y}+\frac{gn^2}{D^{7/3}}N\sqrt{M^2+N^2}=0 \quad (3)$$

The x and y are the rectangular Cartesian coordinates; M and N are the discharge fluxes terms in the x- and y-direction respectively. The fluxes M and N can be expressed as M = u (η+h) = uD and N = v (η+h) = vD; where h is sea depth, η is water elevation above the mean sea level (MSL) and D is the instantaneous depth.

2.2. Numerical model

A staggered scheme is employed for TUNA-M2 as illustrated in figure 1 [6, 15] where the computational locations of the three variables, which are η, u and v (or their associated fluxes M and N) are illustrated.

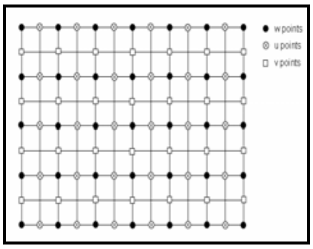

Figure 1. Computational points for a staggered scheme

Partial derivatives are replaced by finite differences as shown in (4), while time step Δt is restricted by the Courant criterion (5) to ensure stability of the numerical scheme.

$$\left(\frac{\partial \eta}{\partial t}\right)_{i,j}^{k+\frac{1}{2}}=\left(\eta_{i,j}^{k+1}-\eta_{i,j}^{k}\right)/\Delta t; \quad \left(\frac{\partial \eta}{\partial x}\right)_{i+\frac{1}{2},j}^{k}=\left(\eta_{i+1,j}^{k}-\eta_{i,j}^{k}\right)/\Delta x \;; \quad \left(\frac{\partial \eta}{\partial y}\right)_{i,j+\frac{1}{2}}^{k}=\left(\eta_{i,j+1}^{k}-\eta_{i,j}^{k}\right)/\Delta y$$

$$\left(\frac{\partial u}{\partial t}\right)_{i+\frac{1}{2},j}^{k}=\left(u_{i+\frac{1}{2},j}^{k+\frac{1}{2}}-u_{i+\frac{1}{2},j}^{k-\frac{1}{2}}\right)\Big/\Delta t \;; \quad \left(\frac{\partial u}{\partial x}\right)_{i,j}^{k+\frac{1}{2}}=\left(u_{i+\frac{1}{2},j}^{k+\frac{1}{2}}-u_{i-\frac{1}{2},j}^{k+\frac{1}{2}}\right)\Big/\Delta x$$

$$\left(\frac{\partial v}{\partial t}\right)_{i,j+\frac{1}{2}}^{k}=\left(v_{i,j+\frac{1}{2}}^{k+\frac{1}{2}}-v_{i,j+\frac{1}{2}}^{k-\frac{1}{2}}\right)\Big/\Delta t \;; \quad \left(\frac{\partial v}{\partial y}\right)_{i,j}^{k+\frac{1}{2}}=\left(v_{i,j+\frac{1}{2}}^{k+\frac{1}{2}}-v_{i,j-\frac{1}{2}}^{k+\frac{1}{2}}\right)\Big/\Delta y \quad (4)$$

$$\Delta t \le \frac{\Delta x}{\sqrt{2gh}} \quad (5)$$

η is water elevation above mean sea level, h is water depth, u and v are the velocities in the x and y direction respectively, g is gravity and t is time. In this paper, distance is measured in meter (m) and time in second (s).

2.3. Open Sea Boundary Conditions

For a study domain containing open sea boundary such as the Indian Ocean, appropriate radiation boundary condition should be implemented in the numerical scheme to allow wave disturbances to pass through the open boundary without reflection. This means that the wave energy can pass through the boundary and travel away from the system to avoid wave reflection, which would otherwise induce disturbances inside the computational domain [5, 7, 10].

2.3.1. Simple Radiation Boundary Condition

A simple radiation boundary condition proposed by Jensen [5] as given by (6) is applied in TUNA-M2 model. By averaging (6a) and (6b), we derive the equation in (6c).

$$\frac{\partial \eta}{\partial t} = 0 \qquad (6a)$$

$$\frac{\partial \eta}{\partial x} = 0 \qquad (6b)$$

$$\frac{\partial \eta}{\partial t} + \frac{\partial \eta}{\partial x} = 0\,. \qquad (6c)$$

A two dimensional numerical implementation of (6c) can be expressed in (7),

$$\eta_{i,j}^{k+1} = \frac{1}{2}\left(\eta_{i,j}^{k} + \eta_{i-1,j}^{k+1}\right) \qquad (7)$$

2.3.2. Modified Orlanski Radiation Boundary Condition

The Modified Orlanski radiation boundary condition is also tested in TUNA-M2. It is observed that this type of radiation boundary condition appears to work well for storm surge simulations [10]. The Modified Orlanski radiation condition is given as (8) and (9).

$$\zeta_B^{n+1} = \zeta_{B-1}^{n} - s\,(\,\zeta_B^{n} - \zeta_{B-1}^{n+1}) \qquad (8)$$

$\hat{s}$ is determined implicitly by,

$$\hat{s} = \frac{\zeta_{B-1}^{n} - \zeta_{B-2}^{n-1}}{\zeta_{B-1}^{n-1} - \zeta_{B-2}^{n}} \qquad (9)$$

where,

$$s = \begin{cases} \hat{s}, & \text{if } \; 0 < \hat{s} < 1, \\ 1, & \text{if } \; |\hat{s}| \geq 1, \\ 0, & \text{if } \; -1 < \hat{s} \leq 0, \end{cases}$$

3 Numerical Testing: Radiation Boundary Condition

A numerical experiment on the two types of radiation boundary condition is tested in a square domain of dimension (0, 40000) by (0, 40000) m^2 in the middle of the ocean. With a depth of 1000 m and the gravitational acceleration of 10 m/s^2, the wave celerity is 100 m/s. An initial displacement defined by the Gaussian hump η=a exp-$(x/\sigma)^2$×exp-$(y/\sigma)^2$ in the form of a circle (figure 2 and figure 3) with given zero initial velocity is created in the middle of the domain. The amplitude of the initial displacement is 10 m whereas σ is 2000 m.

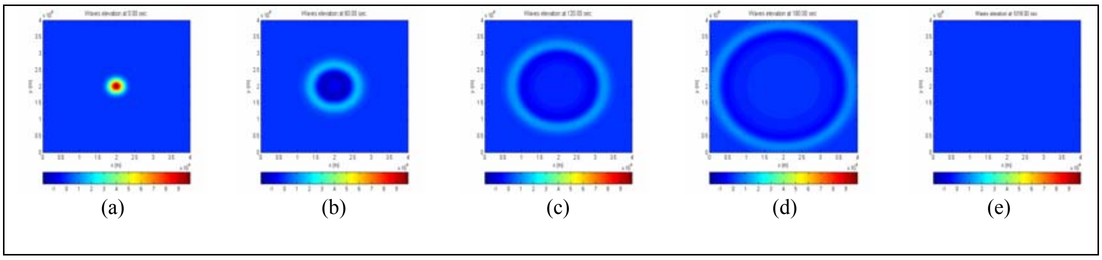

Figure 2: Tsunami propagation in a square with simple radiation condition

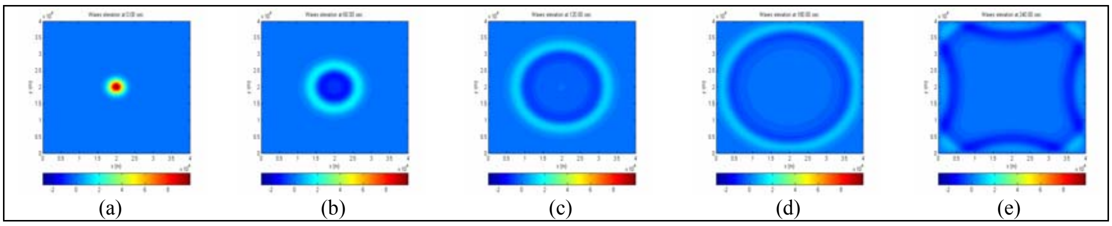

Figure 3: Tsunami propagation in a square with Modified Orlanski radiation condition

As shown in figure 2, the simple radiation boundary condition allows the disturbances to propagate out of the domain through the boundary. However, there are some residual waves remaining inside the study domain after the waves have passed out of the computational domain, due to dispersion of the waves. Similarly, the Modified Orlanski radiation boundary condition also allows the waves to pass through the boundary (figure 3). Compared to the case of figure 2, residual waves remain longer inside the computational domain after the waves have passed out of the computational domain. Hence, simple radiation boundary condition will be used in the study in this paper.

4 December 26 Asian Tsunami in Indian Ocean

Numerical tests have been presented in Teh et al. [11] to indicate that TUNA-M2 simulates hypothetical tsunami propagation correctly and accurately. After some enhancement of radiation boundary condition, TUNA-M2 is then used in the simulation of December 26 Asian tsunami in the Indian Ocean for a computational domain of 1600 km by 2500 km and dx of 2000 m, comprising of 1 million nodes. The contour of the tsunami propagation waves is plotted by MATLAB 6.5. It should be noted that it is time consuming to produce the contour plots for 1 million nodes due to the PC limitation. For computer efficiency, the grid size must be chosen properly in order to obtain adequate resolutions and yet not to impose excessive demand on memory and computational time [11]. The main focus of this simulation is on the wave heights offshore in the vicinity of Sri Lanka, India and Bangladesh (figure 4a). The computational domain chosen is a square of dimension (0, 1600) km x (0, 2500) km, with a grid size of 2000 m, giving rise to a computational grid of dimension 800 by 1250 nodes. The source of initial displacement is composed of an elliptical hump defined by $\eta = a\ \exp(-(x/\sigma_x)^2 \times \exp(-(y/\sigma_y)^2$ where σ_x=42.5 km and σ_y=400 km, indicating a rectangle of dimension 85 km by 800 km [1, 3], with the major axis of 800 km defined by σ_y=400 km in the vertical direction. The initial velocity is given by $u = v = \sqrt{g/2h}\ \eta$ with average Indian Ocean depth, h=3500 m.

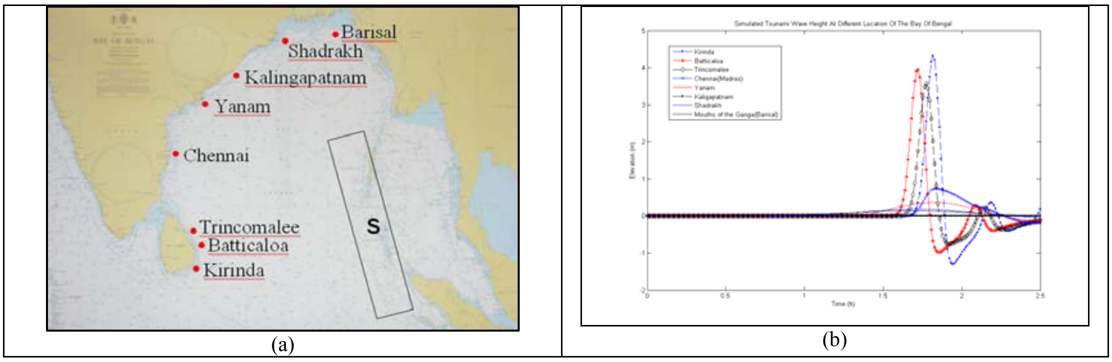

(a) (b)

Figure 4: (a) Map of study domain and (b) Time series of tsunami height at different location in Indian Ocean

Figure 4b shows the time series of tsunami heights at several locations in the Indian Ocean. The coastal areas in Sri Lanka experience the maximum tsunami impact with maximum wave heights of about 4.3 m off the coast in deep water. The simulated wave heights in the offshore coastal areas of India receive waves of less than 1.0 m. The wave height offshore of Chennai is about 0.7 m. On the other hand, Bangladesh only receives refracted waves as it is not located in the main propagation path of the tsunami source. Hence, the tsunami wave height offshore of Bangladesh is about 0.1 m. The reason that Sri Lanka receives the maximum impact is that Sri Lanka lies directly along the path of the main tsunami propagation axis.

The runup heights along beaches may amplify by a factor typically in the range of 2 to 6 [8] depending on a number of contributing factors such as bathymetry and slopes. Table 1 shows the measured runup heights and inundation distances for several locations along the affected regions. For Sri Lanka, the runup height varies from 3 m to 12 m, which is in general agreement with the wave heights offshore of Sri Lanka simulated by TUNA-M2. The runup heights for Chennai are in the range of 1.4 m to 4.8 m, which are consistent with the simulated wave heights of 0.7 m offshore of Chennai.

A series of contours for the propagation of tsunami waves plotted by MATLAB 6.5 is shown in figure 5. The tsunami wave is initiated in figure 5a, propagates westward towards Sri Lanka (figure 5b, c and d) and finally arrives offshore of Sri Lanka (figure 5e) after a travel time of 1.7 hours, with the focus of the wave propagation directed towards Sri Lanka. This is the main reason why Sri Lanka receives the maximum adverse impact of this tsunami. Also quite clear from this diagram is the observation that the tsunami wave propagation hardly reaches

Bangladesh, which is located in the northern most regions in the computational domain.

Table 1. measured runup height

Location	Runup (m)	Inundation distance (m)	Reference
Sri Lanka	<3 to > 12	50 to > 1000	[13]
Chennai	1.4 to 4.8	45 to 200	[9]
Nagapattinam	3.9	750	
Santhankuppam	3.5	80	
Sri Lanka	2.5 to 10	N/A	[14]
Pulicat	3.2	160	[15]
Pattinapakam	2.7	145	
Kovalam	4.3	180	
Kalpakkam	4.1	360	
Periakalapet	3.9	170	
Puttupatnam	2.6	N/A	
Devanaampatnam	2.5	340	
Parangipettai	2.8	700	
Tarangambadi	4.4	400	
Vedaranniyam	3.6	N/A	

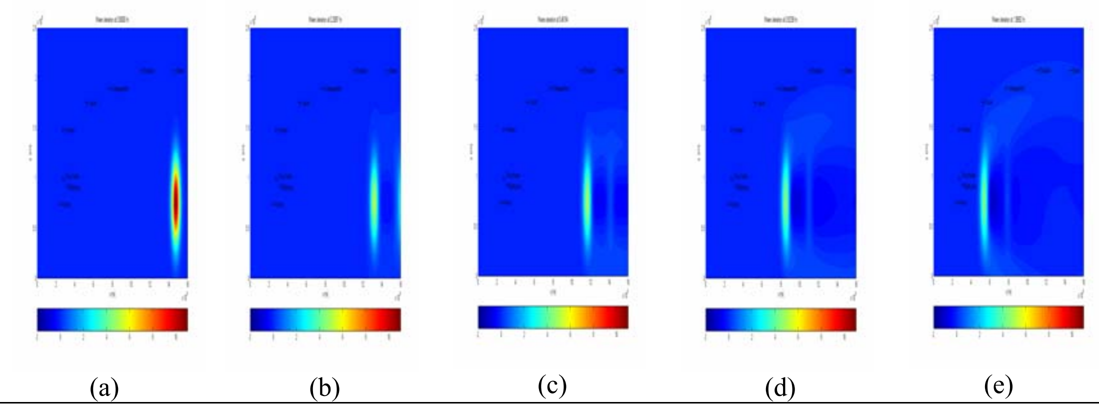

Figure 5. contour of the propagation of tsunami wave (left to right)

5 Conclusion

This paper has presented numerical simulation by TUNA-M2 for tsunami that occurred on 26 December 2004 in the Indian Ocean. A satisfactory radiation boundary condition has been implemented in TUNA-M2 to allow tsunami waves to propagate out of the computational domain through the open boundary. Further, it helps to reduce some numerical defects due to over-dampening especially at coastal boundary. It is hoped that this paper will contribute towards further research on tsunami modeling in future.

6 Acknowledgement

Financial support provided by #304/PMATHS/636034 entitled “A Study of Tsunami Prediction along the Coast of Penang Due to a Source in Sumatra” is gratefully acknowledged.

References

[1] Hérbert, H., Schindelé, F, Altinok, Y., Alpar, B. and Gazioglu, C. Tsunami hazard in the Marmara Sea (Turkey): a numerical approach to discuss active faulting and impact on the Istanbul coastal areas, Marine Geology 215, pp 23-43, 2005.

[2] Imamura, F., Shuto, N. and Goto, C. Numerical simulation of the transoceanic propagation of tsunamis, Paper presented at the Sixth Congress of the Asian and Pacific Regional Division, Int. Assoc. Hydraul. Res., Kyoto, Japan, 1988.

[3] Intergovernmental Oceanographic Commission (IOC). Numerical Method of Tsunami Simulation with the Leap Frog Scheme, 1, Shallow Water Theory and Its Difference Scheme, in Manuals and Guides of the IOC, pp 12-19, Intergovernmental Oceanogr. Comm., UNESCO, Paris, 1997.

[4] Ippen, A. T. Estuary and Coastlines Hydrodynamics: Engineering Societies Monographs. McGraw-Hill Book Company, Inc., 1966.

[5] Jensen, T. G.. Open boundary conditions in stratified ocean models. Journal of Marine Systems 16, pp 297-322, 1998.

[6] Koh, H.L. Environmental and Ecosystem Modeling (Pemodelan Alam Sekitar dan Ekosistem). Universiti Sains Malaysia Publishers, pp 379, 2004.

[7] Koh, H.L., Izani, A.M.I., Teh S.Y., and Cham, K.L. Modeling Tsunami: Towards a Unified Approach For Indian Ocean Tsunami Warning and Mitigation System, Presented at the Workshop on Model Inter-comparison for the Indian Ocean Tsunami, 12-13 December 2005, Hyderabad, India, Invitation of ICG/IOC/UNESCO Intergovernmental Coordinating Group for the Indian Ocean Tsunami Warning and Mitigation System IOTWS, by invitation of ICG/IOTWS, 2005.

[8] Pelinovsky, E., Kharif, C., Riabov, I. and Francius, M. Study of tsunami propagation in the Ligurian Sea. Natural Hazards and Earth System Sciences, vol. 1, pp 195–201, 2001.

[9] Ramanamurthy, M.V., Sundaramoorthy, S., Pari, Y., Ranga Rao, V., Mishra, P., Bhat, M., Usha, T., Venkatesan, R. and Subramanian, B.R. Inundation of sea water in Andaman and Nicobar Islands and parts of Tamil Nadu coast during 2004. Sumatra tsunami. Scientific correspondence. Current Science, India, vol. 88, No. 11, 1736-1740, 2005.

[10] Tang, Y.M. and Grimshaw, R. Recent Development in the Theory and Modelling of Storm Surge: Modelling Coastal and Sea and Processes. World Scientific Publishing Co. The Flinders University of South Australia. pp 135-157, 1999.

[11] Teh, S.Y., Cham, K.L., Koh, H. L. and Izani, A.M.I. Modeling Propagation of the 2004 Tsunami: A Theoretical Analysis. Proceedings of International Conference on Reservoir Operation and River Management, 17 – 19 September 2005, Guangzhou, China, 2005.

[12] Titov, V. V. and Gonzalez, F. I. Implementation and testing of the method of splitting tsunami (MOST). NOAA Technical Memorandum ERL PMEL-112 (contribution no. 1927), 1997.

[13] USGS. The December 26, 2004 Indian Ocean Tsunami: Initial Findings on Tsunami Sand Deposits, Damage, and Inundation in Sri Lanka. Based on Survey Conducted January 9-15, 2005. United States Geological Survey, 2005.

[14] Yalciner, A. C., Pelinovsky, E.N., Kuran, U., Taymaz, T., Zaitsev, A., Ozyurt, G., Ozer, C., Karakus, H., Safak, I., Simulation and Comparison with Field Survey Results of Dec., 26, 2004 Tsunami, 2005.

[15] Yeh, H, Peterson, C., Chadha, R.K., Latha, G., Katada, T. Tsunami Survey along the Southeast Indian Coast. Report #2, Learning from Earthquakes: The Great Sumatra Earthquake and Indian Ocean Tsunami of December 26, 2004. Earthquake Engineering Research Institute (EERI) Special Earthquake Report, 2005.